SCIENCE CHINA
Technological Sciences

November 2010 Vol.53 No.11: 2966–2971
doi: 10.1007/s11431-010-4146-6

Computational and experimental study on dynamic behavior of underwater robots propelled by bionic undulating fins

ZHOU Han, HU TianJiang*, XIE HaiBin, ZHANG DaiBing & SHEN LinCheng

College of Mechatronic Engineering and Automation, National University of Defense Technology, Changsha 410073, China

Received June 16, 2010; accepted August 2, 2010

Bionic undulating fins, inspired by undulations of the median and/or paired fin (MPF) fish, have a bright prospective for underwater missions with higher maneuverability, lower noisy, and higher efficiency. In the present study, a coupled computational fluid dynamics (CFD) model was proposed and implemented to facilitate numerical simulations on hydrodynamic effects of the bionic undulating robots. Hydrodynamic behaviors of underwater robots propelled by two bionic undulating fins were computationally and experimentally studied within the three typical desired movement patterns, i.e., marching, yawing and yawing-while-marching. Moreover, several specific phenomena in the bionic undulation mode were unveiled and discussed by comparison between the CFD and experimental results under the same kinematics parameter sets. The contributed work on the dynamic behavior of the undulating robots is of importance for study on the propulsion mechanism and control algorithms.

bionic underwater robot, CFD, dynamic behavior, undulating fins

Citation: Zhou H, Hu T J, Xie H B, et al. Computational and experimental study on dynamic behavior of underwater robots propelled by bionic undulating fins. Sci China Tech Sci, 2010, 53: 2966–2971, doi: 10.1007/s11431-010-4146-6

1 Introduction

Biomimetic underwater robots have a bright prospect and great potential in both military and civilian applications. The undulating fin propulsion modes inspired by amiiform and balistiform fish are of significance for bionic propulsion research, particularly for the design and control of underwater vehicles [1–12].

According to pioneering studies [13–16], the propulsion mechanism of the bionic underwater robots propelled by undulating fins is unsteady and coupled. In detail, the undulation causes the flow field to change, and vice versa, the concomitant hydrodynamics has effect on the locomotion of bionic underwater robots. Obviously, the relationship between the motions of bionic underwater robots and the flow field is coupled and complicated. And therefore, it is difficult to unveil the coupling process completely by theoretical hydrodynamics.

Generally, the dynamic system model plays an important role in simulation as well as control of underwater vehicles. However, pre-existing theoretical models can be seldom introduced or applied to these bionic underwater robots because of their complex hydrodynamics characteristics [15, 16]. Under such circumstances, an integrated method with computational and experimental approaches is proposed to complement the deficiency of theoretical method in this field. Concretely, a coupled computational fluid dynamics (CFD) model is built to analyze the hydrodynamic effects of the undulating robots, and particularly, the corresponding experiments are carried out to verify whether the CFD numerical results are correct or effective.

*Corresponding author (email: t.j.hu@nudt.edu.cn, tjhu@ieee.org)

2 Materials and methods

In this study, a coupled CFD model was proposed and established with one 6DoF dynamics model of rigid body, one kinematics model of undulating fins and one CFD solver, as shown in Figure 1. The 6DoF dynamics model reveals how the rigid-body underwater robot moves under the hydrodynamic forces, the kinematics model describes the undulating waveform sequences against the time, and finally, the CFD solver is used to compute the hydrodynamic effects caused by the locomotion of the robots. It is understood that the proposed CFD model is coupled with the complex relationships among its components.

2.1 The bionic underwater robot

As shown in Figure 2, the underwater robot is composed of one main body, two undulating fins, two independent caudal fins and other devices. The undulating fins, as the main propeller, are symmetrically distributed on both sides of the vehicle. These two fins can control swimming speed and direction within some horizontal plane with various cooperative modes. Here, the dynamic behavior induced by the undulating fins will be mainly considered.

2.2 The CFD solver

The CFD method is used as numerical approach for hydrodynamic effects during two-fin undulations. As a preprocessing step to construct numerical solution to the underwater robot motion problem, the computation domain discretization has to be accomplished.

The geometry modeling is performed by Solidworks, and the parameters are the same as the physical prototype except that the undulating fins are assumed with zero thickness. The dynamic behavior of the underwater robot is coupled with the undulation of fins and the rigid-body motion of the robot. Therefore, two demands for the mesh model should be considered: 1) the domain is required to be broad enough for the rigid-body space motion; 2) the boundary motion, which results in the dynamic mesh of CFD, includes the two fins' undulation and the rigid-body motion.

Considering the calculation precision and time cost, and in view of the mesh quality better enough during the numerical simulation, the mesh model follows the following principles. 1) A different kind of fluid domain is corresponding to each kind of rigid body motion. 2) The computation domain is divided into two regions, namely inner and outer regions, and the former is meshed with a higher resolution and the latter with a lower resolution.

The coupled CFD model presented in this paper is used to research the dynamic behavior of the undulating robots, furthermore, it can also be used for other kinds of underwater robots.

2.3 The kinematics model of fins

The kinematics model of undulating fins has been established in refs. [17, 18] with the ruled surface as follows:

$$\begin{cases} p_{x_i}(r_i, s_i, t) = s_i, \\ p_{y_i}(r_i, s_i, t) = r_i \cdot d \cdot \cos\left[\theta_{\mathrm{m},i} \cdot \sin\left(\dfrac{2\pi}{T_i}t + \delta_i \dfrac{2\pi}{\lambda_i}s_i + \phi_i\right)\right], \\ p_{z_i}(r_i, s_i, t) = r_i \cdot d \cdot \sin\left[\theta_{\mathrm{m},i} \cdot \sin\left(\dfrac{2\pi}{T_i}t + \delta_i \dfrac{2\pi}{\lambda_i}s_i + \phi_i\right)\right], \\ 0 \leqslant s_i \leqslant L, 0 \leqslant r_i \leqslant 1, \end{cases} \quad (1)$$

where i=1, 2, L is the fin length, d is the uniform length of each fin ray, $\theta_{\mathrm{m},i}$ is the maximal undulation angle, T_i is the undulating period, λ_i is the undulating wavelength, ϕ_i is the initial phase and δ_i decides the direction of wave traveling.

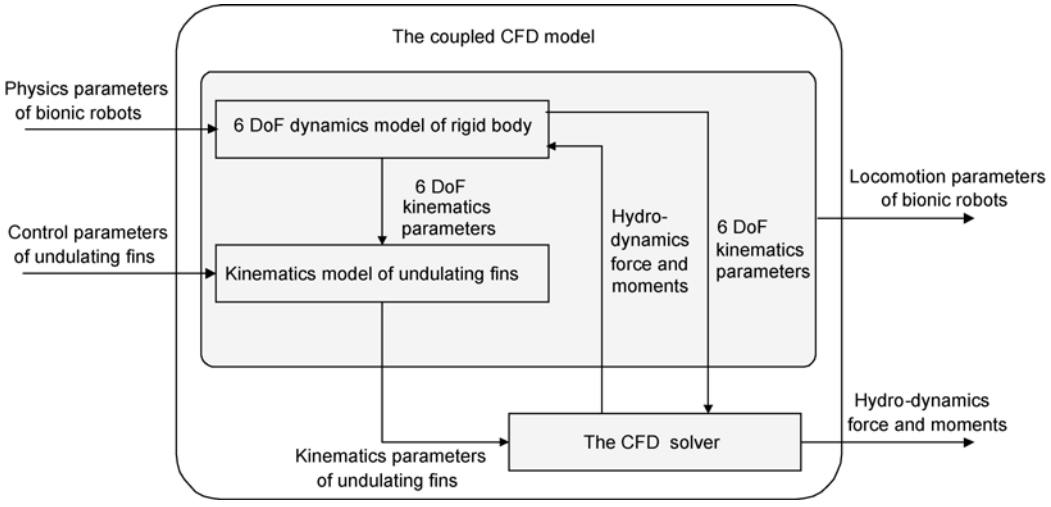

Figure 1 Architecture of the coupled CFD model.

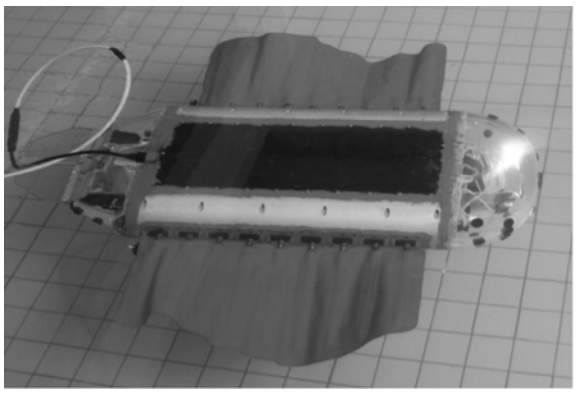

Figure 2 The underwater robot propelled by undulating fins.

δ_i =1 means the wave travels from head to tail, and δ_i =−1 means traveling in the opposite direction. In addition, i=1 means the left undulating fin, while i=2 means the right fin.

2.4 The dynamic model of rigid body

Based on the hydrodynamics of undulating fins [19, 20], the period surge force, lateral force and yaw moment are surely produced during undulations. In the case of one single undulating fin, the period mean of the lateral force or yaw moment is considered to be nearly zero, because of the motion symmetry when the wave number of the undulating fins is an integer. Therefore, the motion of underwater vehicles can be furthermore assumed to be in a horizontal plane. And then, the 6DoF rigid-body dynamics model [21] can be simplified into eqs. (2) and (3). Among them, eq. (2) represents the kinematics equations of the mass center and eq. (3) describes the dynamical equations, respectively.

$$\begin{cases} \dot{x}_e = \dot{x}\cos\psi + \dot{z}\sin\psi, \\ \dot{y}_e = \dot{y}, \\ \dot{x}_e = \dot{z}\cos\psi - \dot{x}\sin\psi, \end{cases} \tag{2}$$

$$\begin{cases} m\ddot{x}_e = T_x, \\ J_y\ddot{\psi} = M_y, \end{cases} \tag{3}$$

where (x_e, y_e, z_e) are the coordinates in the inertial frame, and (x, y, z) are the coordinates in the carrier frame, ψ is yaw angle, m is mass of the underwater robot, J_y is yaw moment of inertia, T_x is the thrust and M_y is yaw moment.

3 CFD study and experimental comparison

Several typical movement patterns were designed for the bionic underwater robots in terms of marching, yawing, and yawing-while-marching on the basis of the aforementioned assumptions on one single undulating fin's hydrodynamics.

3.1 The motion patterns

Marching. If both of the two fins undulate with the same parameters, they will produce identical magnitudes of forces or moments for ideal cases. Furthermore, the directions of forces from the two fins are identical while the directions of moments are opposite apparently. As a result, the net force is a sinusoidal surge force and the yaw moments can almost be counteracted.

In this marching pattern, the kinematics parameters are given by

$$\theta_{m,1} = \theta_{m,2};\ T_1 = T_2;\ \lambda_1 = \lambda_2;\ \ \phi_1 = \phi_2;\ \delta_1 = \delta_2 = 1. \tag{4}$$

Yawing. If the fins undulate with the same parameters except that the wave traveling directions are opposite, then the magnitudes of forces and moments are identical. Furthermore, the directions of forces from two fins are opposite while directions of moments are the same. Therefore, the net forces can be thought to be counteracted.

In the yawing pattern, the kinematics parameters can be expressed as follows:

$$\theta_{m,1} = \theta_{m,2};\ T_1 = T_2;\ \lambda_1 = \lambda_2;\ \ \phi_1 = \phi_2;\ \delta_1 = 1,\ \delta_2 = -1, \tag{5}$$

$$\theta_{m,1} = \theta_{m,2};\ T_1 = T_2;\ \lambda_1 = \lambda_2;\ \ \phi_1 = \phi_2;\ \delta_1 = -1,\ \delta_2 = 1. \tag{6}$$

Note that eq. (5) corresponds to the right-turn yawing, and eq. (6) to the left-turn yawing.

Yawing-while-marching. There are several methods to realize the yawing-while-marching motion, such as different undulating frequencies, different undulating amplitudes and different wavelengths. This paper implemented this pattern with different frequencies. The undulation with a larger frequency results in a surge force with a larger mean value [19, 20]. Therefore, surge forces of different amplitudes will be generated by the two fins, and the yawing-while-marching motion will be induced by this dynamic feature.

In the yawing-while-marching pattern, the kinematics parameters are designed as follows:

$$\theta_{m,1} = \theta_{m,2};\ T_1 < T_2;\ \lambda_1 = \lambda_2;\ \ \phi_1 = \phi_2;\ \delta_1 = \delta_2 = 1, \tag{7}$$

$$\theta_{m,1} = \theta_{m,2};\ T_1 > T_2;\ \lambda_1 = \lambda_2;\ \ \phi_1 = \phi_2;\ \delta_1 = \delta_2 = 1. \tag{8}$$

Note that eq. (7) corresponds to a right-turn yawing-while-marching, and eq. (8) to a left-turn yawing-while-marching.

Through the CFD simulation, the locomotion of bionic robots and the hydrodynamics characteristics of flow field were obtained for each given undulation pattern. Moreover, the results from experiments and simulation with the same kinematics parameters were also compared in the following sections.

3.2 Marching

Numerical simulation of marching was done by using the coupled CFD model. As for comparability, the kinematics parameters in both computation and experiments were set as the same; see Table 1.

In the CFD study, the kinematic and dynamical variables

Table 1 Parameters for the desired three motion patterns

	Parameters	Units	Marching		Yawing		Yawing-while-marching
			Set-1	Set-2	Set-3	Set-4	Set-5
Left fin	T_1	s	1	0.5	1	2	2/3
	$\theta_{m,1}$	(°)	15	15	15	15	15
	ϕ_1	(°)	0	0	0	0	0
	λ_1	m	0.6	0.6	0.6	0.6	0.6
	δ_1	-	1	1	1	1	1
Right fin	T_2	s	1	0.5	1	2	2
	$\theta_{m,2}$	(°)	15	15	15	15	15
	ϕ_2	(°)	0	0	0	0	0
	λ_2	m	0.6	0.6	0.6	0.6	0.6
	δ_2	-	1	1	−1	−1	1

were all in accordance with the given undulation. After the start period, the mean of surge force decreased with time, and the convergent form was a quasi-sinusoid with a nearly zero mean. Since the robot mass was barely changeable, the acceleration had the similar tendency. The velocity increased and developed towards a quasi-sinusoid with a stationary periodic average value and slight amplitude. The trends of surge force and velocity under Set-1 in Table 1 were shown by the red dotted and blue solid lines in Figure 3. Moreover, the mean of convergent velocity was nearly 0.5 m/s, and the acceleration lasted 18 s approximately. The mean of convergent velocity was nearly 1.0 m/s under the parameter Set-2 in Table 1.

The locomotion sequences with parameter Set-1 from both computation and experiments were presented in Figure 3. The CFD figures are colored by pressure magnitude. These sequences were sampled at the same given points and were correspondingly arranged. The comparison between computational and experimental results showed that the movements under the coupled CFD model just coincided with practice. Therefore, the proposed CFD model was validated to be effective in the marching pattern. In the experiments, an acceleration process was also found in marching swimming motion of underwater robots. The maximum speed was about 0.45 m/s and the acceleration occupied nearly 20.0 s under parameter Set-1 in Table 1. As for parameter Set-2 in Table 1, the maximum speed was about 0.9 m/s and the acceleration period lasted nearly 18.0 s. The characteristics of accelerating and converging were confirmed in accordance with the CFD and experimental phenomena. So was the trend of the stationary velocity going with undulating frequencies.

3.3 Yawing

The two parameter sets for computation and experiments on the yawing motion were listed as Set-3 and Set-4 in Table 1. It was observed that in the CFD simulation, the developing process of yaw moment was analogous to the surge force in the marching pattern. The trends of yaw moment and angular velocity under Set-3 were shown by the red dotted and blue solid lines in Figure 4. After the start period, the absolute average value of yaw moment tended to decline along with the undulation time, and the yaw moment approached to some nearly zero-mean quasi-sinusoid form. At the same time, the angular velocity approached to some specific form with a steady mean and a small amplitude. Therefore, in the CFD simulation, as soon as the fin started undulating, the robot started yawing motion, then the angular velocity became larger and larger, and finally the underwater robot kept yawing with some steady angular velocity. The change regularities were analogous within the other parameters sets. Moreover, the steady angular velocity was about 1.00 rad/s under parameter Set-3 and 0.47 rad/s by using parameter Set-4 in Table 1.

The locomotion sequences with the parameter sets of the yawing motion from both computation and experiments were correspondingly presented in Figure 4. The CFD figures are colored by pressure magnitude. The experimental results coincided with the CFD calculation, indicating the validity of the coupled CFD model. The convergent steady angular velocity in the experiment was 0.79 rad/s under parameter Set-3 and 0.27 rad/s under Set-4 in the table. Like the marching pattern, some similar phenomena were also found in the yawing pattern by comparing experimental results with computational results. In detail, the characteristics of angular velocity increasing and converging were confirmed in accordance with the two approaches. So was the trend of the convergent value of angular velocity varying with undulating frequencies.

3.4 Yawing–while-marching

The parameter sets for yawing-while-marching motion in numerical simulation and experiments were listed in Set-5 of Table 1. In the CFD simulation, it was found that the mean of surge force decreased with the time, and the surge force approximated to zero-mean quasi-sinusoid form in the end. The forward velocity increased to a stable value, while the lateral velocity increased at first, then decreased, and finally tended to zero-mean. The yaw moment was negative (namely clockwise), and the absolute mean value decreased with the time. Moreover, the yaw moment also approximated to some zero-mean quasi-sinusoid regularity in the end.

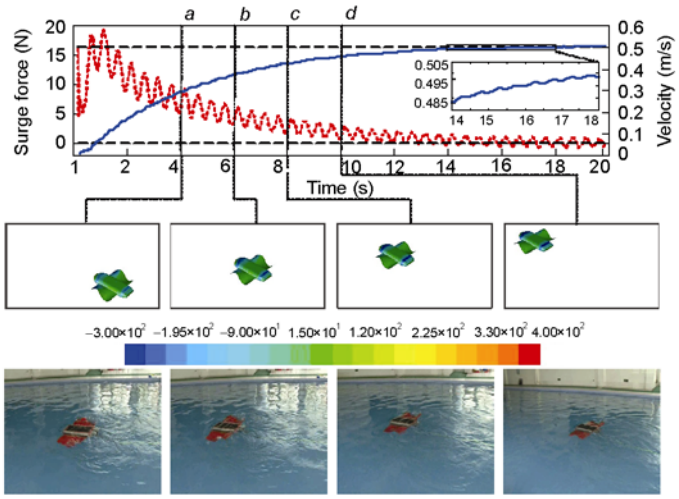

Figure 3 Computational and experimental results for marching pattern.

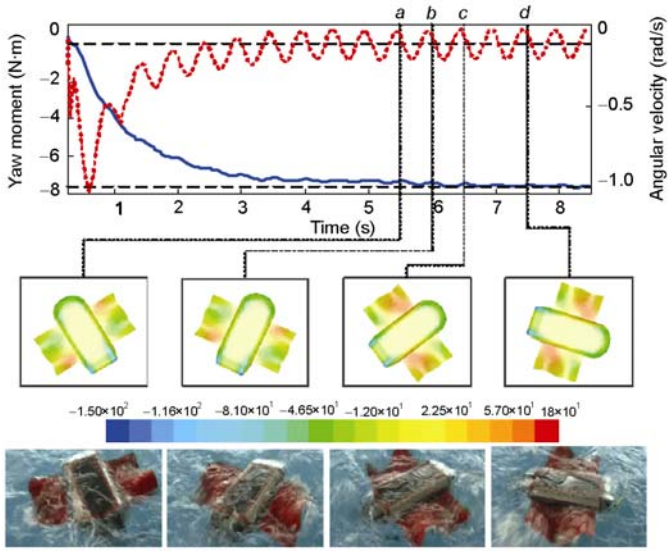

Figure 4 Computational and experimental results for yawing pattern.

The developing process of yaw moment was similar to the surge force, but the convergence rate was faster than that of surge force. The absolute value of yaw angular velocity increased to a relatively stable value of nearly 0.57 rad/s. In Figure 5, the robot's motion trajectory in the horizontal plane was shown by the red dotted line, and the trend of yaw angle was described by the blue solid line. The dynamic motion also coincided between the computational and experimental results within the yawing-while-marching pattern, as shown in Figure 5. Moreover, the CFD figures are colored up by pressure magnitude.

4 Conclusions

In this paper, the coupled CFD model was established for the study on dynamic behavior of underwater robots propelled by two undulating fins. This computational model is composed of 6DoF dynamics model of rigid body, the kinemics model of undulating fins and the CFD solver. Significantly, hydrodynamic behaviors have been jointly studied via both computational and experimental approaches within the desired three undulation patterns, i.e., marching, yawing, and yawing-while-marching.

Several phenomena were unveiled and discussed in this paper. For instance, in the marching pattern, the mean of surge force decreased with the time, and the convergent form was a quasi-sinusoid whose mean was nearly zero. This conclusion is different from the study on fin-base-fixed cases [18]. In addition, the trend of convergent value of angular velocity going with undulating frequencies is the same [19, 20]. Moreover, the coupled CFD model has been

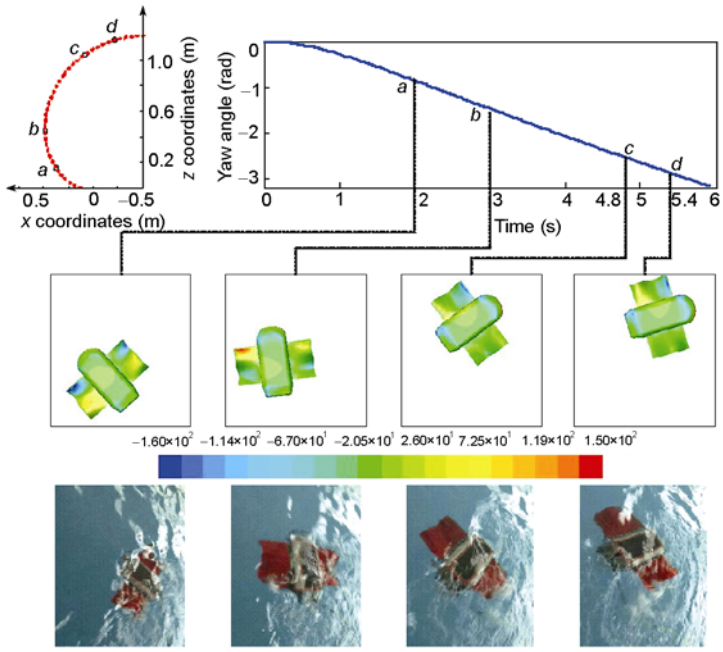

Figure 5 Computational and experimental results for yawing-while-marching pattern.

validated by experiments.

The work has formed a meaningful basis of computational platform for future studies on the propulsion mechanism and control algorithm of bionic underwater robots. Eventually, this platform will also be useful for other kinds of underwater robots that have complicated interactions with fluid environment.

This work was supported by the National Natural Science Foundation of China (Grant No. 60805037). The authors would like to thank XU HaiJun, LIN LongXin and WANG Gang for their sincere help to this manuscript.

1 Bandyopadhyay P R. Biology-inspired science and technology for autonomous underwater vehicles. IEEE J Ocean Eng, 2004, 29(3): 542–546
2 Bandyopadhay P R, Castano J M, Rice J Q, et al. Low speed maneuvering hydrodynamics of fish and small underwater vehicles. J Fluid Eng, 1997, 119: 136–144
3 Bozhurttas M, Tangorra J, Lauder G, et al. Understanding the hydrodynamics of swimming: From fish fins to flexible propulsors for autonomous underwater vehicles. Adv Sci Technol, 2008, 58: 192–202
4 Hu T J, Shen L C, Low K H. Bionic asymmetry: From amiiform fish to undulating robotic fins. Chin Sci Bull, 2009, 54(4): 562–568
5 Yoseph B C. Biomimetics—Using nature to inspire human innovation. Bioinspir Biomimet, 2006, 1(1): 1–12
6 Sfakiotakis M, Lane D M, Davies B C. An experimental undulating-fin device using the parallel bellows actuator. In: IEEE Internatioal Conference on Robotics and Automation, 2001, Seoul, Korea
7 Epstein M, Colgate J E, MacIver M A. A biologically inspired robotic ribbon fin. In: IEEE/RSJ International Conference on Intelligent Robots and Systems, Workshop on Morphology, Control, and Passive Dynamics, 2005, Edmonton, Canada
8 Low K H. Design, development and locomotion control of bio-fish robot with undulating anal fins. Int J Robot Auto, 2007, 22(1): 88–99
9 Hu T J, Shen L C, Lin, L X, et al. Biological inspirations, kinematics modeling, mechanism design and experiments on an undulating robotic fin inspired by gymnarchus niloticus. Mech Mach Theory, 2009, 44(3): 633–645
10 Zhang Y H, He J H, Zhang S W, et al. Research on biomimetic fish fin driven by NiTi shape memory alloy (in Chinese). Robot, 2007, 39(3): 207–213
11 Low K H. Modelling and parametric study of modular undulating fin rays for fish robots. Mech Mach Theory, 2009, 44(3): 615–632
12 Toda Y, Ikedab H, Sogihara N. The motion of a fish-like underwater vehicle with two undulating side fins. In: The Third International Symposium on Aero Aqua Bio-mechanisms (ISABMEC 2006), 2006, Ginowan, Japan
13 Bandyopadhyay P R. Maneuvering hydrodynamics of fish and small underwater vehicles. Integrat Comp Biol, 2002, 42: 102–117
14 Triantafyllou M S, Hover F S, Techet A H, et al. Review of hydrodynamic scaling laws in aquatic locomotion and fishlike swimming. Appl Mech Rev, 2005, 58: 226–236
15 Xie H B，Shen L C. Collaborative modeling of underwater vehicle dynamic system (in Chinese). J Syst Simul, 2007, 19(9): 2130–2133
16 Xie H B，Zhang D B, Shen L C. Collaborative simulation based on MATLAB/Simulink and FLUENT (in Chinese). J Syst Simul, 2007, 19(8): 1824–1827
17 Wang G M, Shen L C, Hu T J. Kinematic modeling and dynamic analysis of the long-based undulation fin of gymnarchus niloticus. In: The 9th International Conference on the Simulation of Adaptive Behavior, 2006, Roma, Italy
18 Hu T J. Undulation adaptability theory and control for the biomimetic undulating fins (in Chinese). Dissertation of Doctoral Degree. Changsha: National University of Defense Technology, 2008
19 Shirgaonkar A A, Curet O M, Patankar N A, et al. The hydrodynamics of ribbon-fin propulsion during impulsive motion. J Experim Bio, 2008, 8: 3490–3503
20 Zhou H, Hu T J, Xie H B, et al. Computational hydrodynamics and statistical modeling of biologically inspired undulating robotic fins: A two-dimensional study. J Bio Eng, 2010, 7(1): 66–76
21 Xie H B. Design, modeling, and control of bionic underwater vehicle propelled by multiple undulatory fins (in Chinese). Dissertation of Doctoral Degree. Changsha: National University of Defense Technology, 2006